Pergamon

Cement and Concrete Research, Vol. 26, No. 2, pp. 243-251, 1996

0008-8846/96 $15.00 + .00

SSDI 0008-8846(95)00211-1

THE CaO DISTRIBUTION TO MINERAL PHASES IN A HIGH CALCIUM FLY ASH FROM EASTERN GERMANY

Michael Enders
WWU - Institut für Mineralogie Corrensstr. 24 48149 Münster Germany

(Refereed)
(Received August 21, 1995; in final form November 6, 1995)

ABSTRACT

High Calcium Fly Ashes (HCFA) are increasingly important as an admixture to mortar and concrete. The reactivity of HCFA is related to mineral phases like free lime, glassy spheres, anhydrite and yee'liminite. The occurrence of CaO in several crystalline phases and at least one non-crystalline mineral phase complicates the quantification of any of those mineral phases. This study focuses on an direct assessment of free lime and an indirect method for determination of CaO bounded in glassy spheres and anhydrite. CaO is enriched in fine particle size ranges. Glassy spheres are the most important CaO bearing mineral phase in the examined HCFA. The maximum CaO content bound in a glassy matrix is close to the composition of anorthite (< 25 wt%). This is probably due to the restricted solubility of chemical species in a cooling melt of anorthitic composition. At the end of the high temperature process an equilibrium is attained between free lime, anhydrite and glassy spheres. The distribution of CaO among mineral phases is controlled by the availability of SO_3 and free lime.

Introduction

High calcium fly ashes (HCFA) are well known for their cementing properties. They are classified by the American Society for Testing and Materials (ASTM) as Class C fly ash, and they are characterized by a combined pozzolanic and hydraulic reaction with water (1). These cementing properties are associated with reactive mineral phases. The most prominent reactive mineral phases are glassy spheres, free lime, anhydrite and yee'liminite (2, 3, 4).

The quantification of reactive mineral phases with easy accessible analytic procedures is difficult. This is consequence of the incorporation of reactive chemical species in several mineral phases and the occurrence of crystalline and non-crystalline mineral phases which complicate quantitative XRD-procedures. Free lime and anhydrite can be determined with routine wet chemistry, XRF and XRD procedures. The content of glassy material has been assessed with various methods. Former workers tried to determine the amount of glassy spheres from the amorphous hump in X-Ray diffraction pattern, by difference from XRD-spectra or by

differential wet chemical analysis (4, 5, 6). These methods can not differentiate glassy spheres of varying composition. Recent work confirmed a variable composition of single glassy spheres in HCFA (2, 7, 8). A CaO content > 25 wt% is characteristic of very reactive glassy spheres (8). Computer Controlled SEM (CCSEM) has been used to determine the chemical composition of single particles in large populations (9). This method is restricted by overlapping of X-Ray excitation volumes of micronsized particles. Light and electron microscopy are very time consuming, and they can not be applied for routine analysis. Cathodoluminescence in combination with EDX-spectrometry might be valuable for future work to distinguish rapidly particles of varying reactivity (10).

This study focuses on the determination of CaO-bearing mineral phases from combined wet chemistry analysis and XRF-analysis. The data can be used to calculate the fraction of total CaO bound in free lime, anhydrite and glassy spheres. As the reactivity of glassy material rises with increasing CaO content, these data might help in evaluating the reactivity of HCFA with routine analytic procedures. Yee'liminite - a reactive mineral phase described from HCFA (2, 8) is a minor constituent, and it will be neglected in this approach.

Methods

HCFA-samples were taken from the electrostatic precipitators of a power plant south of Leipzig, Germany. This plant uses a pulverized high calcium lignite fuel, which formed in a

TABLE 1

Representative Major Element Analysis of Fly Ash Samples
(Block II: VR, MR, NR, Block III: MA Bottom Ash)
All data in wt%. MA stands for fly ash blend from VR, MR and NR

Block stage	bottom-ash	II VR	II MR	II NR	III MA
SiO_2	46.39	41.98	35.36	30.47	54.58
TiO_2	0.64	1.38	1.48	1.08	1.28
Al_2O_3	9.83	21.67	22.34	16.73	16.28
Fe_2O_3	7.37	6.73	6.36	6.46	7.31
MnO	0.05	0.13	0.14	0.16	0.09
MgO	1.14	1.91	2.14	2.37	1.36
CaO	11.58	21.50	25.11	27.87	15.63
Na_2O	0.09	0.13	0.12	0.26	0.12
K_2O	0.33	0.42	0.42	0.44	0.47
P_2O_5	0.14	0.14	0.17	0.15	0.10
SO_3	8.36	3.53	4.53	14.10	3.20
LOI	nd	0.70	1.10	3.10	0.50
sum	85.92	100.26	99.25	103.19	100.92
CaO(f)	0.40	1.70	1.80	1.00	0.70

nd - not determined

continental environment. The major mineralogic constituents in the raw coal are quartz, kaolinite, marcasite, pyrite and gypsum (8, 11). CaO-bearing mineral phases other than gypsum are sparse in the raw lignite coal. This observation implies organic material as the major calcium source. Inside the combustor maximum temperatures reach 1250°C. Local temperatures on the surface of burning coal particles probably exceed this value.

The fly samples for this study were taken from different consecutive stages (VR, MR, NR) of the electrostatic precipitators from several boilers (II, III, IV) in the power plant during sampling periods in spring 1991 and summer 1992. The major mineralogic composition of the fly ash samples comprise quartz, glassy spheres (+ minor anorthite and gehlenite), anhydrite, free lime, iron oxides and yee'liminite (8). The representative chemical analysis of the fly ash samples are given in table 1.

The fly ash samples were size fractionated using a dry sieving procedure (> 100 μm, 63-100 μm, 45-63 μm, 32-45 μm, 20-32 μm, < 20 μm). The sieving process was optimized and supervised in terms of sieving time, sample size and vibration speed with a Malvern MS20 lasergranulometer. The particle size distribution of single size fractions was determined with the lasergranulometer. The D10-data from the particle size distribution correlated well with chemical data (FIG.1). The D10 parameter is therefore used to describe the variation of chemical composition with grain size. The D10 and D90 data from the lasergranulometric data was identical to the nominal width of the limiting sieve apertures. Particle sizes exceeding (commonly less than 10 %) the nominal width of the sieves are probably a residue of incomplete separation or the occurrence of non-spherical particle morphologies or a shift of single sieve apertures from the nominal width.

Each size fraction was analyzed with wet chemical analysis and XRF spectrometry. The free lime content was titrated according to ASTM C114. It was important to mill the material carefully to give the titration fluid access also to free lime encapsulated in glassy material (7). The SO_3 content, the total CaO content and the Al_2O_3 content of the samples were determined with a Siemens SRS 200 XRF-spectrometer from pressed pellets. The calibration line was based on 38 fly ash standards. Further XRF and XRD results for single size fractions will be reported elsewhere.

The variation of chemical data with grain size data is presented graphically using binary plots of chemical data versus D10 of single size fractions.

Results

Chemical Data. The variation of chemical data with grain size is depicted in FIG. 1. FIG. 1A displays total CaO of size fractions versus D10 from the lasergranulometric grain size determination. CaO increases with decreasing particle size. This is well known from many HCFA (7, 12). It was possible to express the relation between D10 and CaO content in linear ($Y=mx+b$) and exponential functions ($Y=e^{(a+bx)}$). The results are listed in table 2. The resulting factors are similar for all fly samples independent of the sampling point and sampling time and major element composition of the bulk samples (comp. table 1). First, this confirms a constant composition of the examined fly ash samples in relation to grain size over a one year period. Second, these data indicate a constant process governing the CaO distribution to mineral phases in HCFA. The functions for both models are almost congruent. The higher correlation coefficients for the exponential model indicate the overlaying influence of several mineral phases on the CaO distribution in the fly ash samples.

TABLE 2

Results of Regression Analysis CaO vs. D10. A - linear model, B - exponential model. Roman numbers indicate a single boiler of the power plant. VR, MR and NR mark consecutive stages of the electrostatic precipitator. MA stands for fly ash blend from VR, MR and NR

linear	Y-intercept	A slope	R^2
II-VR	33.33	-0.20	98.71
II-MR	32.24	-0.21	99.19
II-NR	30.17	-0.22	98.72
III-MA	27.90	-0.19	94.76
IV-MA	33.22	-0.20	98.64
exponential	**a**	**B b**	**R^2**
II-VR	3.58	-0.01	99.75
II-MR	3.53	-0.01	99.70
II-NR	3.41	-0.01	99.62
III-MA	3.53	-0.01	99.47
IV-MA	3.56	-0.01	99.54

SO_3 is highly enriched in fine grained particles (FIG. 1B). There are two sources for sulfur in the raw coal. First iron sulfides are oxidized. This process leads to iron oxides and SO_2 in the flue gas. This SO_2 may react with CaO set free from organic material and O_2 to form anhydrite (eq. 1). Second gypsum, decomposes during the high temperature process to SO_2, oxygen and free lime. After the high temperature process SO_2 from the flue gas reacts with free lime and O_2 to anhydrite (eq. 1). Anhydrite nucleates preferentially on surfaces of rapidly cooling small particles. The condensation of anhydrite is amplified by the cumulative effect of high surface area of small particles and their faster cooling rates compared to larger particles.

$$CaO + SO_2 + \tfrac{1}{2} O_2 <===> CaSO_4 \quad (1)$$

In FIG 1B three data points are marked as agglomerates. Single particles from those size fractions were separated and examined with a Debye-Scherrer XRD-camera. Those separates turned out to consist mostly of bassanite. This observation confirms a partial hydration of anhydrite to bassanite and a partial agglomeration of SO_3 rich fine grained particles. These data points are shifted parallel to abscissa towards coarse D10 values. These agglomerates were not ruptured during the sieving process.

The relation of free lime versus D10 is displayed in FIG. 1C. Free lime is enriched in fine grained particles. Maximum values reach up to 3.5 wt%. Some very fine grained size fractions display a decrease in the free lime content. The CaO-determination according to ASTM C114 can not discriminate free lime from portlandite. This codetermination of free lime and portlandite with ASTM C114 excludes a hydration reaction of free lime to portlandite as a possible mechanism for the observed CaO(f) decrease in fine particles. The decrease of CaO(f) in fine particles can only be explained with a reaction using free lime. The most likely

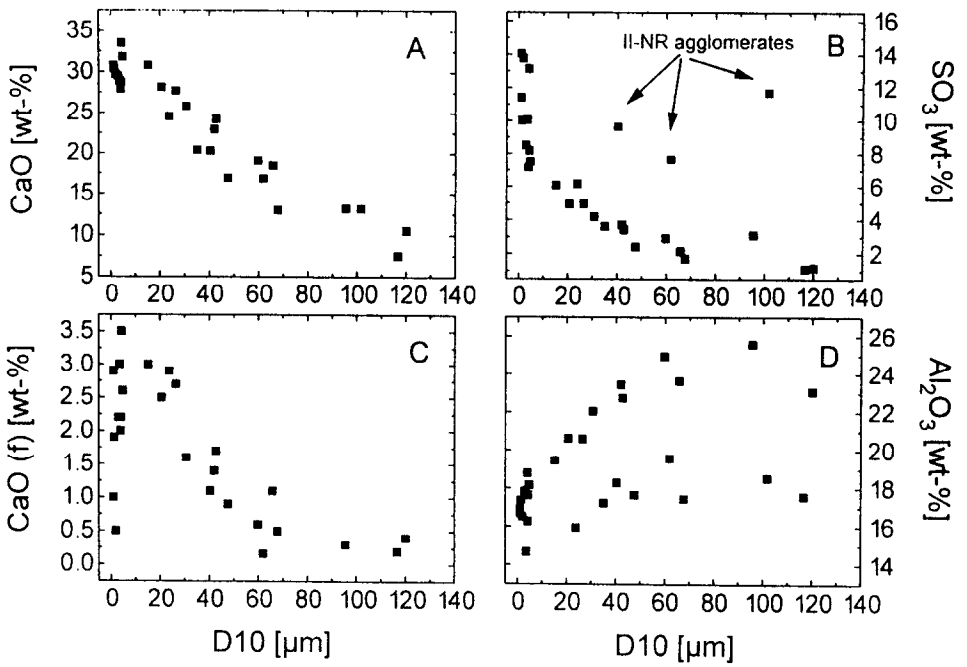

FIG. 1.
Variation of total CaO vs. D10 (A), SO_3 vs. D10 (B), free lime vs. D10 (C), and Al_2O_3 vs. D10 (D). D10-data taken from lasergranulometer data for size fractions.

candidates for CaO consuming reactions are the formation of glassy spheres from free lime and alumino silicate melt or the reaction of free lime with SO_2 via $CaSO_3$ to anhydrite (eq.1). From the following discussion the latter seems to be more probable.

Glassy spheres stem from clay minerals in the raw coal (2, 8). In the examined fly ash samples glassy spheres are the most important Al_2O_3 bearing mineral species (8). Therefore the Al_2O_3 content of size fractions is indicator for the amount of glassy spheres in the fly ash sample. FIG 1D indicates a decrease of aluminium towards fine grained size fractions. This is due to a marked increase of SO_3 and CaO, which diminishes the relative importance of Al_2O_3.

CaO Partitioning in Mineral Phases. Figure 1 outlined the behavior of chemical species with grain size. These data can be used to determine the calcium oxide bounded in glassy spheres according to (eq. 2)

$$CaO(g) = CaO(t)\text{-}CaO(f)\text{-}CaO(s)\ [wt\%] \quad (2)$$

where CaO(t) is the total CaO from XRF analysis, CaO(f) is the free lime of size fractions from titration according ASTM C114, CaO(s) is the anhydrite bounded CaO calculated from the SO_3 of XRF-analysis (eq. 3), CaO(g) is the calcium oxide fixed in glassy spheres.

$$CaO(s) = 0.7006 * SO_3\ [wt\%] \quad (3)$$

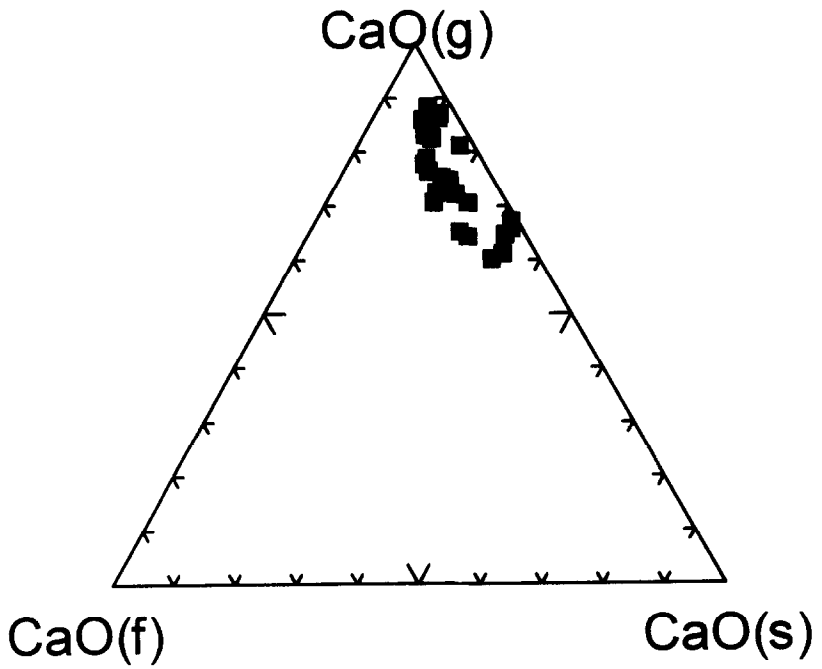

FIG. 2.
Ternary diagram with CaO assigned to glassy spheres CaO(g), free lime CaO(f) and anhydrite CaO(s) at the apices.

The resulting data can be used to construct a ternary diagram with CaO(g), CaO(f) and CaO(s) at the apices (FIG. 2). The data points of all size fractions cluster in the high CaO(g) corner of the diagram. The distribution of the data points is independent of particle size. This behavior can be interpreted as an "equilibrium" which is attained between free lime, anhydrite and glassy spheres. Further, these data can be used to construct binary diagrams of CaO(s) vs. CaO(g) and CaO(s) vs. CaO(f) (FIG. 3).

First, it is obvious from FIG. 3A, that CaO(g) increases with increasing CaO(s). FIG. 1B confirmed an increase of SO_3 with decreasing particle size. CaO(s) is directly related to SO_3 and therefore increasing CaO(s) represents a decrease in particle size. The value of CaO(g) is an average CaO content of all glassy spheres of single size fractions. The increase of CaO(g) in FIG. 3A indicates, that either the CaO content of a given number of glassy spheres changes with particle size, or that the absolute amount of glassy material with a constant CaO increases with decreasing particle size. From FIG. 1D the latter seems to be less probable, because Al_2O_3 as a major constituent of glassy spheres decreases with decreasing particle size. Further Enders (8) showed for the same samples, that the composition of glassy spheres strictly follows a kaolinitic ratio of SiO_2/Al_2O_3.

Any of these possible explanations leads to the same conclusion of an increased amount of reactive particles in the fine particle range. This observation complies well with the qualitative results of former workers who found an increased reactivity in fine grained HCFA (6, 11).

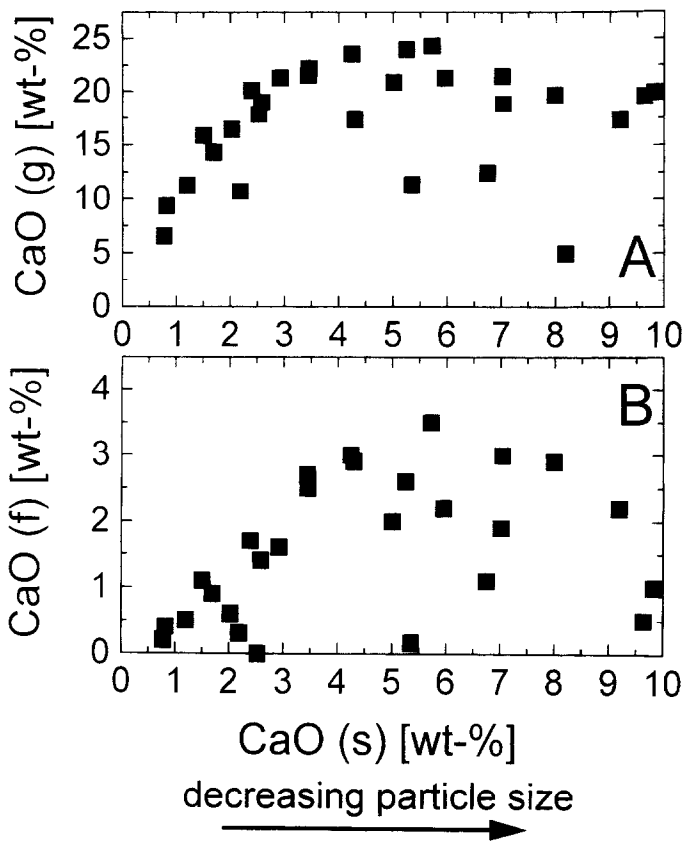

FIG. 3.
Variation of CaO(g) (A) and CaO(f) (b) versus CaO(s).

FIG. 3A shows a maximum of CaO(g) at 25 wt%. This value was former reported as the lower limit in CaO content for highly reactive glassy spheres (8). This boundary is close to the CaO content of crystalline anorthite (20.15 wt%) in the ternary diagram of $CaO\text{-}SiO_2\text{-}Al_2O_3$. An explanation for this boundary for CaO incorporation in glassy material could be the structural similarity of anorthitic melts and anorthite (13). This similarity leads to an increased polymerization rate in a anorthitic melt inhibiting the solubility of CaO in the melt.

When CaO(g) attains a value of approximately 25 wt% no further increase can be observed. This point is also the onset for a rapid increase of CaO(s). The flattening curve for CaO(g) can be interpreted as the end of the high temperature process. The cooling melt reached a final CaO rich composition, and the condensation of anhydrite on cooling particles becomes the more important process (comp. FIG. 1 C).

The diagram for free lime shows a increase of free lime with increasing CaO(s) (FIG. 3B). At 3.5 wt% CaO(f) reaches a plateau. The onset of the plateau coincides with the plateau in the CaO(g) vs. CaO(s) diagram (FIG. 3A). With a further increase of CaO(s) CaO(f) stays constant or even decreases slightly. The flattening curves in FIG. 3A and FIG. 3B mark the ending

supply of CaO for glassy material and free lime. This mark can interpreted as the end of CaO liberation from organic material and the end of the combustion process. The slight decrease with further increasing CaO(s) is probably be due to the reaction of SO_2 and free lime to anhydrite (eq. 1). This reaction is restricted to fine grained particles with large surface areas (FIG. 1C).

Conclusions

Glassy spheres are a very important factor in the setting mechanisms of hydrated HCFA. The reactivity of single fly ash particles increases with the CaO content of the particle (8). As it is impossible to determine the chemical composition of all glassy spheres one has to approximate the composition with other methods. FIG 1 outlined the variation the major chemical species of reactive mineral phases with particle size (CaO, free lime, SO_3 and Al_2O_3). The data for two calcium bearing chemical species and the total CaO in the sample can be used to calculate also the CaO fixed in glassy spheres. Independently from particle size most calcium oxide is bounded to glassy spheres (FIG. 2). Anhydrite and free lime are enriched in fine grained particles (FIG. 1B, FIG. 1C). Only free lime particles in the submicron range react with SO_3 to form anhydrite. The rather constant distribution of CaO among free lime, anhydrite and glassy spheres suggests a kind of "equilibrium" between these mineral phases (FIG. 2). The maximum CaO content of glassy spheres is limited to 25 wt%. This value also marks a major boundary in reactivity, as reported by (8). This value coincides with results from Kumm & Scholze (13), who found a close structural relation between anorthitic melts and anorthite leading to high crystallization rates. Glassy spheres with CaO > 25 wt% probably contain free lime inclusions (8). The exchange of CaO between several mineral phases is inhibited, when anhydrite starts to form in a cooling environment and the CaO solubility is limited in a highly polymerized melt. Only partially free lime is consumed by excess SO_2 to form additional anhydrite.

The reactivity of HCFA is controlled by the occurrence of reactive mineral phases. Reactive mineral phases comprise mainly Ca-bearing mineral phases. This study might help developing methods to evaluate and to optimize HCFA for the usage as an admixture to mortars and concretes.

Acknowledgement

This paper is part of a Ph-D-Thesis, which was conducted on behalf of Prof. Dr. H.-U. Bambauer at the Westfälische-Wilhelms-Universität, Münster. I thank Prof. Bambauer for many stimulation discussions and his guidance throughout the last years.

References

1. Hellmuth, R., Fly ash in cement and concrete, Portland cement Assoc. Skokie, Illinois (1987)
2. McCarthy, G.J., Johansen, D.M., Thedchanamoorthy, A., Steinwand, S.J., Swanson, K.D., Mat. Res. Soc. Proc. 113, 99 (1988)
3. McCarthy, G.J., Manz, O.E., Johansen, D.M., Steinwand, S.J., Stevenson, R.J., Mat. Res. Soc. Proc. 86, 109 (1986)

4. Diamond, S., Cement and Concrete Research 13, 459 (1983)
5. Querol X., Fernandez Turiel, J.L. & Lopez Soler, A., Min. Mag 58, 119 (1994)
6. Schreiter, P., Silikattechnik, 19, 358 (1968)
7. Pöhl, K., Zur Konstitution and Hydratation deutscher Braunkohlenfilteraschen, Ph-D thesis, Leipzig, (1994)
8. Enders, M., Cement and Concrete Research 25, 1369 (1995)
9. Miller, S.F.& Schobert, H.H., Energy Fuels 7, 520 (1993)
10. Münch, U. & Götze, J., Abfallwirtschaft 6, 772 (1994)
11. Zschach, S., Chem. der Erde 37, 330 (1978)
12. Enders. M. (1994): Mineralogisch/Chemische Untersuchungen an Braunkohlenfilteraschen aus dem Leipziger Revier (KW Thierbach), Ph-D thesis, Münster, (1994)
13. Kumm, K.A., Scholze, H., Tonindustrie-Zeitung and Keramische Rundschau 93, 332